

# Estimators of primary energy and mass at UHE

Jean-Noël Capdevielle\*

\*APC, Univ. Paris-Diderot and IN2P3-CNRS, 10 rue A.Domon et L.Duquet, 75205 Paris Cedex 15

**Abstract. The data of AGASA is amended in both steps of energy conversion (treatment of inclined showers and analysis of the vertical equivalent shower). A general agreement with GZK prediction is confirmed.**

**Keywords: GZK prediction, UHE EAS**

## I. INTRODUCTION

After proposing an appropriate treatment for inclined showers, we pointed out a general reduction of the intensity measured at AGASA [1]; we investigate here the effect of the fluctuations on the conversion from vertical density  $S_{600}(0)$  (measured at 600m from axis) to the primary energy.

## II. ENERGY ESTIMATORS FOR GIANT SURFACE ARRAYS

At ultra high energy, the primary energy  $E_0$  (in eV) is recovered for the most recent data with the conversion of AGASA [2]:

$$E_0 = 1.96 \cdot 10^{19} \left( \frac{S_{600}(0)}{100} \right)^{1.02} \quad (1)$$

A different procedure than in AGASA is followed in AUGER [3], where the primary energy is derived from the density  $S_{38^\circ}$  at 1000 m distance:

$$E_0 = 1.49 \cdot 10^{17} (S_{38^\circ})^{1.078} \quad (2)$$

( $S_{38^\circ}$  is expressed here in Vertical Muon Equivalent (VME)). It appears convenient to describe analytically the typical histograms derived from our M.C. simulation with CORSIKA by the Extreme value distributions (E.V.D.) taking into account the specific asymmetries of the distributions obtained for  $S_{600}(0)$ . The E.V.D. probability density function for the density  $S$  at fixed primary energy has the form:

$$f(S) = \frac{1}{\sigma} \exp \left( \pm \frac{\mu - S}{\sigma} - e^{\pm \frac{(\mu - S)}{\sigma}} \right) \quad (3)$$

where the parameters  $\mu$  and  $\sigma$  are related to the average size  $\bar{S}$  and its variance  $V_S$  by  $\bar{S} = \mu \pm 0.577 \sigma$  and  $V_S = 1.645 \sigma^2$ . An example is shown on fig.1a in the case of 80 near vertical showers observed at AGASA level (protons of energy  $10^{20}$ eV) with  $\bar{S}_{600} = 304.9$  and  $V_{S_{600}} = 38.94$ ; the left wing is populated by young showers interacting deeper in the atmosphere (in relation with the energy cross section) whereas the right wing consists of older showers submitted to a more important cascading. The relation between the vertical estimator  $S_{600}(0)$  and the primary energy is also

submitted to the response of the detectors, the accuracy in the core localisation, the dependance on hadronic interaction models and on primary composition. All those factors interact together, more or less weighted by the differential energy spectrum in regard to the observable used to classify the EAS, electron size, muon size, densities taken as estimators, fluorescence and Cerenkov light. The Monte Carlo simulations suggest that the fluctuation of the electron density at 600 or 1000m sampled for a large number of shower can be described by a  $\Gamma$  distribution (4):

$$f(S) = \frac{a(aS)^{b-1} \exp(-aS)}{\Gamma(b)} \quad (4)$$

with an average  $\bar{S}$  and its variance  $V_S$  defined by  $\bar{S} = \frac{b}{a}$  and  $V(S) = \frac{b}{a^2}$ , the maximum being obtained for  $S = \frac{b-1}{a}$ . The corresponding situation in the case of AGASA is illustrated by the densities reconstructed on fig.1b (average error on axis position 30m, accuracy on density 10%). The profile of the distribution of  $S_{600}$  (used hereafter for  $S_{600}(0)$ ) at fixed primary energy is strongly distorted by the errors on density measurements and on the localization of the shower core; it moves from an E.V. D. distribution to a distribution more asymmetric with a characteristic increase of the right wing. We have assumed a root mean square deviation of 10., 20., 30., 40., 50.m. on the axis determination, a relative r.m.s. of 10% on density and a dependence of the density at  $r = 600m$  in  $r^{-3.8}$  ([4]. The final profile can be described analytically by a Lognormal ([5]) or a Gamma distribution adopted here (table I).

TABLE I  
S600 DISTRIBUTION FOR  $E_0 = 10^{20}$ EV, DEPENDENCE ON AXIS LOCALIZATION AND DENSITY MEASUREMENT

$\Delta(r), \Delta(S)$	$\langle S_{600} \rangle$	$\sigma$
0., 0.	304.9	38.94 <sup>1</sup>
0., 10%	304.8	39.2
10.m, 0.%	306.8	42.8
10.m, 10%	307.0	53.58
20.m, 0.%	310.1	55.07
20.m, 10%	308.9	63.58
30.m, 0.%	315.7	74.44
30.m, 10%	316.4	82.8
40.m, 0.%	324.3	95.6
40.m, 10%	322.0	99.8
50.m, 0.%	326.5	113.0
50.m, 10%	327.2	119.2

<sup>1</sup>E.V.D. distribution ( $\Delta(r) = 0.$ ) Gamma distribution ( $\Delta(r) \geq 10.$ )

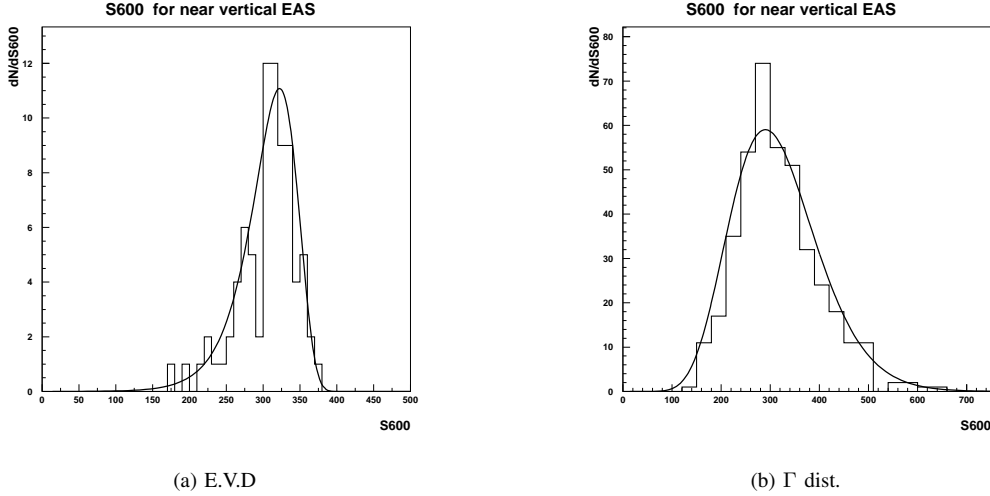


Fig. 1. Monte Carlo fluctuations of S600 fitted by the Extreme Variable Distribution (left). The same fluctuations after introduction of errors on density measurements and axis localisation (right).

### III. PRIMARY ENERGY DISTRIBUTION FOR A FIXED VALUE OF THE ESTIMATOR

Using in quality of statistic weight the differential primary energy spectrum  $J(E) = A E^{-\gamma}$ , it is possible to evaluate the average primary energy associated to a fixed value S600 as:

$$\langle E \rangle = \frac{\int_{E_1}^{E_2} f(E, S600) J(E) dE}{\int_{E_1}^{E_2} J(E) dE} \quad (5)$$

$f(E, S600)$  is the probability for an energy E to generate a shower with a given value for S600, corresponding to a Gamma distribution where the relation between S600 and E has been derived from our Monte Carlo simulations at  $E_0 = 10^9, 5 \cdot 10^9, 10^{10}, 5 \cdot 10^{10}, 10^{11}$  GeV ( $S$  and  $V(S)$  have been parametrized versus the primary energy). The significative energy interval contributing to S600 in equation 5 is shown on fig.2a for a fixed index  $\gamma = 3$ . at all energies (solid line) for a fixed value  $S600 = 200$ . A discontinuity in the energy distribution as a sharp knee or ankle (fig2) generates respectively an overestimation or an underestimation of the average energy associated to S600 when compared to a situation with a fixed index  $\gamma = 3$ . The position of the knee has been fixed here at  $E_0 = 5.623 \cdot 10^{19}$  eV. We can observe how the contribution of ultra energetic primaries falls in the same circumstance for  $S600 = 300$ . on fig.3 for  $\gamma = 5$ . near  $10^{20}$  eV. In order to understand the consequences of more realistic spectra, we have adapted the fits used by [6] and [7] in the analytic descriptions:

$$J(E_0) = A \times \left( \frac{E_0}{E_c} \right)^{-\gamma} \quad (6)$$

with  $\gamma = 3.26, 2.81, 5.1$  respectively for  $E_0 \leq E_c = 10^{18.65}, 10^{19.75}$  eV and also for  $E_0 \geq 10^{18.65}$  eV

$$J(E_0) = A \times \left( \frac{E_0}{E_c} \right)^{-\gamma} \times \frac{1}{1 + \exp\left(\frac{\lg(E_0) - \lg(E_c)}{W_c}\right)} \quad (7)$$

where  $\gamma = 2.56$ ,  $E_c = 10^{19.75}$  eV and  $W_c = 0.16$ . The dip for both spectra is close to  $10^{18.65}$  eV.

The overestimation on the primary energy estimation of near vertical showers becomes more and more important for energies above the "GZK knee" taken at  $5.623 \cdot 10^{19}$  eV as it can be seen on fig.4 for different efficiencies in axis localization. It may be ascertained that the discrepancies are small (when both spectra 6 (dotted-dashed) and 7 (dashed) are involved); the overestimation increases systematically after entering in the knee region together with primary energy and inaccuracy on axis localization.

### IV. THE TREATMENT OF INCLINED EAS

Thanks to the large solid angle of collection, the most important part of the data is concerned by inclined EAS. The most probable density at the distance selected for the estimator (600 m for AGASA, 1000 m for AUGER) is derived from the best analytic distribution fitted to the densities on the detectors. In the case of AGASA, the density  $\rho_{600}(\theta)$  is used to determine  $S_{600}(\theta)$  which is in turn converted to the value of the estimator for shower generated by the same primary Cosmic Ray particle (S600 in the previous section) at vertical incidence. We have shown that the absorption of  $S_{600}(\theta)$  is not exponential; the previous conversion extrapolated from lower energies has been the source of an important overestimation of S600 and therefore of  $E_0$  [1]. This conversion inferred by fitting the attenuation of  $S_{600}$  was

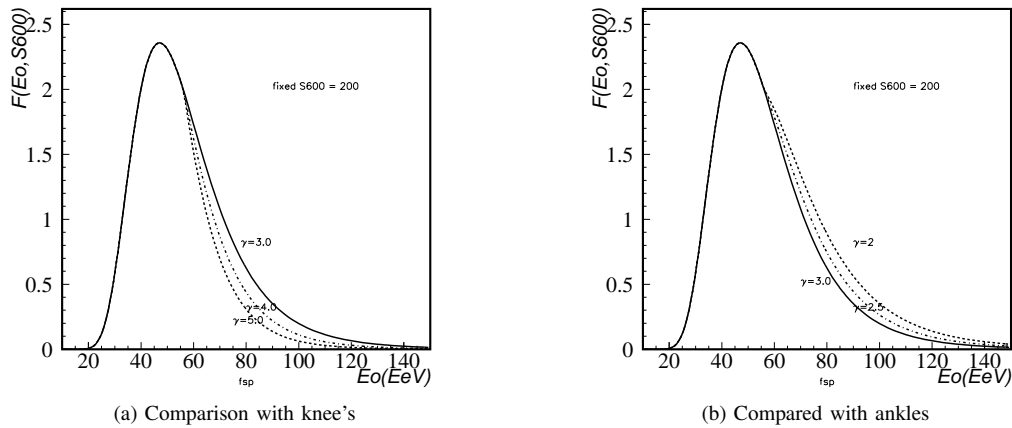


Fig. 2. Energy distributions corresponding to  $\gamma = 3$ . for fixed  $S600 = 200$ .. The circumstances knee(left for  $\gamma = 4., 5.$ ) and ankle (right for  $\gamma = 2.5, 2.$  turns to a decrease or an increase of the value  $\langle E \rangle$  corresponding to  $S600 = 200$ ..  $F(Eo, 600) = f(E, 600)J(Eo)$

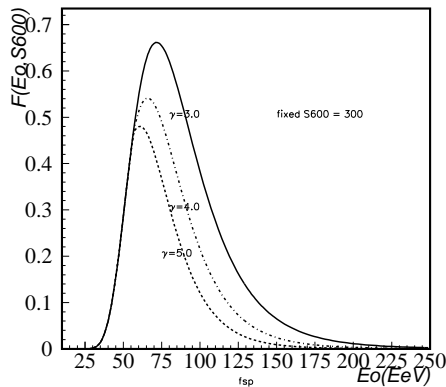


Fig. 3. Primary energy distribution for fixed  $S600 = 300$ .

represented by:

$$S_{600}(\theta) = S_{600}(0) \exp\left(-\frac{t_0}{\Lambda_1}(\sec(\theta) - 1) - \frac{t_0}{\Lambda_2}(\sec(\theta) - 1)^2\right) \quad (8)$$

Constant values  $\Lambda_1 = 500 \text{ gcm}^{-2}$  and  $\Lambda_2 = 594 \text{ gcm}^{-2}$  have been employed in AGASA.

The Fig. 5 exhibits the relative dependence of the electron densities (at 600 m) on zenith angle derived from our simulation.

The dotted line (bottom) represents the AGASA conversion of particle density at 600 m from zenith angle  $\theta$  to the corresponding value for vertical shower (formula 8). The simulations at ultra high energy contradict the classical absorption behaviour of relation 8 (the lowest line in Fig. 5): for the highest energies the density  $\rho_{600}(\theta)$  increases progressively in function of the primary energy versus  $\sec(\theta)$  reaching a maximum between  $10^\circ - 20^\circ$  and then decreases with zenith

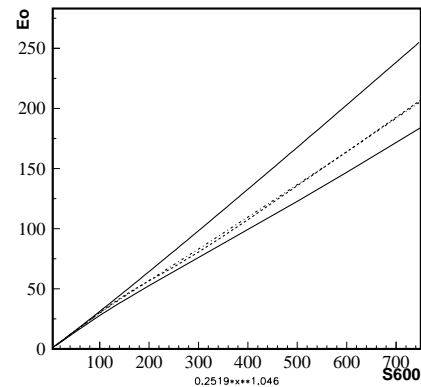


Fig. 4. Overestimation of the average primary energy  $Eo$  (in EeV) for near vertical EAS taking into account the statistical effects of the knee and the accuracy of the axis determination. From top, conversions of  $S600$  to primary energy, respectively following AGASA procedure (solid line), taking into account spectra 6 (dotted-dashed) and 7 (dashed) for  $\Delta(r) = 30\text{m}$  and  $\Delta(S) = 10\%$ , lower line for spectrum 7,  $\Delta(r) = 50\text{m}$  and  $\Delta(S) = 10\%$

angle for primary protons ( $E_0 = 10^9, 5 \cdot 10^9, 10^{10}, 5 \cdot 10^{10}, 10^{11} \text{ GeV}$ ). The dependence shown in Fig. 5 is a general consequence of the electromagnetic cascade theory. This typical behaviour can be described analytically by the so called distorted gaussian function:

$$f(l) = A \times \exp\left(\frac{k}{8} - \frac{s\delta}{2} - \frac{1}{4}(2+k)\delta^2 + \frac{1}{6}s\delta^3 + \frac{1}{24}k\delta^4\right) \quad (9)$$

where:  $l = \sec(\theta)$ ,  $\delta = (l - \langle l \rangle) / \sigma$ . (parameters in Formula 9 are tabulated in [1].

## V. THE CONVERGENCE TO GZK PREDICTION

Both steps of the procedure used in AGASA contribute to the apparent divergence between AGASA data

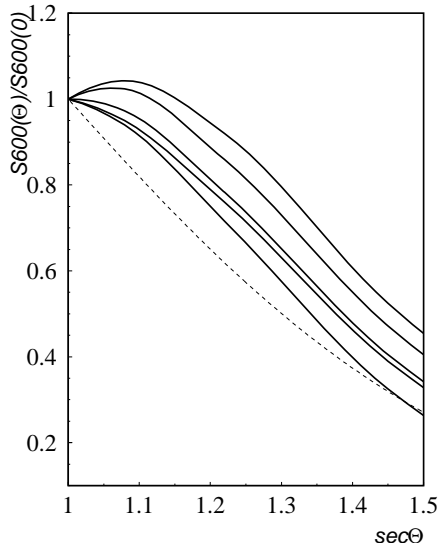


Fig. 5. Dependence  $\frac{S600(\theta)}{S600(0)}$  versus  $\sec(\theta)$  for protons with  $E_0 = 10^9, 5 \cdot 10^9, 10^{10}, 5 \cdot 10^{10}, 10^{11}$  GeV for model QGSJET01

and HIRES or AUGER measurements. AUGER escaped to the difficulties of AGASA ; the density of reference at a zenith angle of  $38^\circ$  at 1000m from axis is more stable (larger contribution of muons than in AGASA and corrections with hybrid events). We have amended in table II the most energetic events of AGASA applying the reduction factors Rv (for the vertical shower) and Ra (treatment of inclined cascades) determined from the previous sections. Rv is given for 30m and 50m assuming a relative r.m.s. on densities of 10%, Eag and  $\theta$  are the energy and the zenith angle of the event, E(30) and E(50) are the energy amended. A case of amendment

TABLE II  
PRIMARY ENERGY AMENDED FOR 11 MOST ENERGETIC EVENTS IN AGASA

Eag	$\theta(^{\circ})$	Ra	Rv(30)	Rv(50)	E(30)	E(50)
10.1	39	1.50	1.22	1.29	5.52	5.22 <sup>2</sup>
21.3	22	1.24	1.24	1.38	13.92	13.44
13.4	36	1.49	1.23	1.31	7.26	6.82
14.4	14	1.10	1.23	1.32	10.60	9.86
10.5	34	1.43	1.23	1.29	5.96	5.68
15.0	44	1.62	1.23	1.33	7.52	6.96
12.0	27	1.30	1.22	1.30	7.56	7.10
10.4	35	1.45	1.22	1.29	5.86	5.51
12.2	24	1.24	1.22	1.30	8.68	7.56
24.6	37	1.60	1.24	1.39	12.36	11.60
12.1	22	1.21	1.22	1.22	8.19	7.70

of the primary spectrum of AGASA is also presented on fig.6 together with the data of AUGER and HIRES. : this preliminary energy reduction was carried as in [1] assuming a random distribution of the zenith angle inside  $45^\circ$ , a determination of the axis with an r.m.s. of 30m and an accuracy of 10%. After consideration of maximum depth and absorption in AUGER [1], a

<sup>2</sup>zenith angle was restored by J.S. with a code of Gamma ray Astronomy [1] from the data of AGASA (date, R.A. declination)[8]

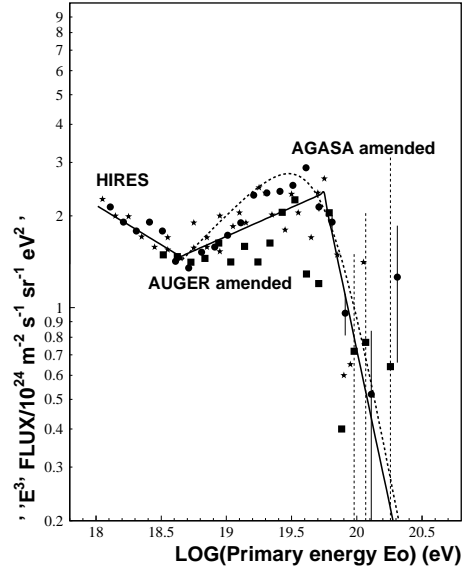


Fig. 6. AGASA spectrum amended (squares) compared to HIRES (stars) and AUGER (discs) data (energy increased by 12%)

general increase of energy by 12% has been applied for AUGER spectrum, HIRES data remaining unchanged. We have also observed that in addition to the maximum depth and the muon electron abundance (correlated to the primary mass, but also to other interaction features, first of all the cross section and the multiplicity) the ratio of the fluorescence light emitted in the upper part of the cascade (respectively near  $500 \text{ gcm}^{-2}$  and  $1100 \text{ gcm}^{-2}$ ) is about twice for an iron primary than for a proton. The cascade profile of the most energetic cascade of HIRES [9] looks in favour of a majority of proton primaries at UHE. For all those reasons, we consider that AGASA data is in agreement with GZK prediction, as well as the measurements of HIRES and AUGER.

#### REFERENCES

- [1] J.N. Capdevielle, F. Cohen, B. Szabelska, J. Szabelski, J.Phys.G, 2009 and references herein (in the press)
- [2] K. Shinozaki, inv. talk, XIV ISVHECRI, Weihai, (2006)
- [3] M. Roth, Pierre Auger Collaboration, Proc. 30<sup>th</sup> ICRC, Merida 313 (2007)
- [4] J.N. Capdevielle, C. Le Gall, J. Gawin, I. Kurp, B. Szabelska, J. Szabelski and T. Wibig, Nuovo Cimento 25C 393, 424 (2002).
- [5] J.N. Capdevielle et al., Proc. 20th ICRC, Moscow, 5, 430 (1987)
- [6] D. Bergman, 30<sup>th</sup> ICRC, Merida, 1128 (2007)
- [7] T. Yamamoto, Pierre Auger Collaboration, Proc. 30<sup>th</sup> ICRC, Merida 318 (2007)
- [8] <http://www-akeno.icrr.u-tokyo.ac.jp/AGASA/results.html#100EeV>
- [9] P. Sokolsky, inv. talk, XV ISVHECRI, Paris, (2008)